Chemie der Erde 78 (2018) 490–499

Contents lists available at ScienceDirect

Chemie der Erde

journal homepage: www.elsevier.com/locate/chemer

Carbon and nitrogen pools in Padanian soils (Italy): Origin and dynamics of soil organic matter

C. Natali[a], G. Bianchini[a,*], L. Vittori Antisari[b], M. Natale[b], U. Tessari[a]

[a] Department of Physics and Earth Sciences, University of Ferrara, Italy
[b] Department of Agricultural and Food Sciences, Alma Mater Studiorum, University of Bologna, Italy

ARTICLE INFO

Handling Editor: M Barbieri

Keywords:
Agricultural soils
C-N isotopes
Organic and inorganic pools
SOM dynamics

ABSTRACT

Carbon and nitrogen elemental (C-N, wt%) and isotopic (δ^{13}C-δ^{15}N, ‰) investigation has been carried out on alluvial and deltaic soils from the Padanian plain (northern Italy), an area interested by intensive agricultural activities, to refine previous inferences on depositional facies, pedogenetic processes and anthropogenic influences. Soil analysis, carried out by EA-IRMS, have been focused on inorganic and organic fractions properly speciated by a thermally-based method, whereas further insights on the organic matter constituents have been obtained by sequential fractionation. The bulk EA-IRMS analyses reveal a remarkable compositional heterogeneity of the investigated soils (TC 0.89 to 11.93 wt%, TN 0.01 to 0.78 wt%, $\delta^{13}C_{TC}$ -1.2 to -28.2‰, δ^{15}N -1.2 to 10.0‰) that has to be explained as an integration between inorganic and organic pools. The latter have been subdivided in Non-Extractable Organic Matter (NEOM, δ^{13}C -16.3 to -28.6‰) and in extractable fractions as Fulvic (FA, δ^{13}C -24.7 to -27.5‰, δ^{15}N 0.6 to 5.7‰) and Humic (HA, δ^{13}C -24.6 to -27.0‰, δ^{15}N 1.0 to 9.7‰) Acids, which have been used to infer soil dynamics and Soil Organic Matter (SOM) stability processes. Results indicate that SOM at depth of 100 cm was generally affected by microbial reworking, with the exception of clayey and peaty deposits in which biological activity seems inhibited. Peaty and clayey soils display an organic fraction loss of ca. 20% toward the surface, suggesting deterioration possibly induced by intensive agricultural activities. These latter may be the cause of the ubiquitous losses of organic fraction throughout the investigated area over the last seventy years, evaluated by the comparison with historical data on corresponding topsoils. The obtained insights are very important because these soils are carbon (and nitrogen) sinks that are vulnerable and can be degraded, loosing agricultural productivity and potentially contributing to greenhouse gases fluxes.

1. Introduction

The Padanian Plain (northern Italy), is the sedimentary basin bordered by the Alps and the Apennines, which hosts about 30–40% of the Italian population and most of the Nation's industrial and agricultural activities. The geochemistry of its sediments records an interplay of tectonic, climatic and hydrological processes. These sediments have been investigated by several papers which were mainly focused on the inorganic constituents that represent useful proxies to understand the provenance of the clastic particles and the relationships with the depositional environment (Amorosi et al., 2002; Bianchini et al., 2002; Amorosi, 2012; Bianchini et al., 2012, 2013; 2014; Di Giuseppe et al., 2014a, 2014b). However, most of these papers never described the associated organic fraction which is fundamental to understand the occurring pedogenetic processes, and only few works discussed the role of the organic matter in soils and sediments from nearby areas (Di Giuseppe et al., 2014c; Migani et al., 2015). In this framework, this paper aims to complement the previous investigations providing systematic carbon and nitrogen elemental and isotopic analyses of soils from the easternmost Padanian plain. In particular, inorganic (TIC) and organic (TOC) soil carbon pools have been characterised by EA-IRMS on the basis of their thermal behavior (Natali et al., 2018). The Soil Organic Matter (SOM) has been investigated separating the non-extractable and extractable components (humin, humic and fulvic acids; Ciavatta et al., 1990), which have been analysed for their C and N elemental and isotopic composition. The presented data are essential to define the C-N pools coexisting -at different extent- in the distinct sedimentary facies, and to understand the biogeochemical cycles occurring in the investigated environmental-agricultural system (*cfr.,* Six et al., 2002; Amundson et al., 2003;Paul, 2014). The data provide insights on organic matter dynamics and transformation and allow to estimate the soil nutrient storage capacity in relation to the existing

* Corresponding author at: Dept. of Physics and Earth Sciences, University of Ferrara, via Saragat 1, 44122, Ferrara, Italy.
E-mail address: bncglc@unife.it (G. Bianchini).

https://doi.org/10.1016/j.chemer.2018.09.001
Received 4 May 2018; Received in revised form 6 July 2018; Accepted 10 September 2018
0009-2819/ © 2018 Elsevier GmbH. All rights reserved.

agricultural activities. The approach is also useful to evaluate the SOM evolution and the related effects on carbon sequestration and/or greenhouse gases release of the investigated soils (e.g. Albaladejo et al., 2013; Ogrinc et al., 2015).

2. Geo-pedological and land use framework

The soils of the easternmost Padanian Plain developed from alluvial (and deltaic) deposits; they are characterised by a limited profile development, in which the lack of soil maturity is related to young depositional age (Holocene), fluvial reworking and extensive agricultural activities (ploughing). In the studied area, located in the neighbours of the town of Argenta (province of Ferrara), the outcropping sedimentary facies (and the related soils) reflect climatic changes and human impacts that deeply modified the configuration of the local drainage system, which is mainly represented by the migrating branches of the Po river (Bondesan et al., 1995; Stefani and Vincenzi, 2005; Simeoni and Corbau, 2009). In the same sector of the plain, sediments of Apennine provenance transported in historical times by River Reno are also represented, giving further complexity to the geomorphological evolution of the plain, in turn reflected in the sediment stratigraphy. In the terminal part of the basin the delta environment was characterised by high lateral mobility of the active channel belts, with recurrent avulsion and channel bifurcation, which redistributed the water and sediment fluxes throughout the system. This dynamic scenario permitted, in historical times, the development of fens and swamps, sometimes characterised by peat deposition (Di Giuseppe et al., 2014a, 2014b). Some of these wetlands possibly received sedimentary contributions from both the Po and Reno riverine systems, as already observed in other sectors of the easternmost Padanian plain (Bianchini et al., 2014). This geomorphological evolution implies that the parent material of the studied soils was heterogeneous, leading to the formation of a variety of different soils.

The studied soils belong to the Inceptisols order and their classification highlights their origin from reclamation land. The predominant group is Aquic Haplusteps (17 soil samples), followed by Udifluventic Haplustept (8 soil samples), Sulfic Endoaquepts (6 soil samples), then Vertic Endoaquepts (3 soil samples). Entisols are also recognized as Oxyaquic Ustifluvents (Soil Survey Staff -SSS, 2010). Pedological features and soil taxonomy is reported in Supplementary Table 1.

The land uses thematic maps of the Emilia-Romagna region reveals that most of the samples are representative of arable lands mainly devoted to cereal crops, with few exceptions of orchards (sampling sites 18, 19 and 28), tree plantations (sampling site11) and humid areas (sampling site 38).

3. Investigated materials and analytical methods

3.1. Soil samples

The samples considered in this study were sampled in the year 2009 and preliminarily studied by Di Giuseppe et al. (2014d), which presented a complete set of major and trace element analyses carried out by X-Ray Fluorescence (XRF). The samples were collected around the town of Argenta (44°36′47″N, 11°50′11″ E; Fig. 1). At each sampling site two samples were collected: one close to the surface (labelled *A*) representative of the plough horizon (just beneath the roots zone; depth 20–30 cm) and the other representative of the underlying undisturbed layer (depth 100–120 cm, labelled *B*). The rationale behind this sampling strategy is that the *A* samples potentially record effects of anthropogenic activities, whereas *B* samples better represent the local background. A subset of 47 soil samples, dried and stored in sealed PTE bags, were reconsidered for carbon and nitrogen analyses in the year 2012. In particular, 38 *B* samples were selected to investigate the C and N background, at a depth not affected by mechanical disturbance. For 11 selected sites, the study of the above mentioned subsoils was coupled with that of the respective superficial layer in order to account for the effect of agricultural practices (ploughing, fertilizers and crops). Moreover, textural analyses were carried out on a subset of samples and the related results are reported in Supplementary Table 2.

3.2. EA-IRMS analysis

The elemental and isotopic carbon composition of the different carbon and nitrogen pools were carried out by the use of an Elementar Vario Micro Cube Elemental Analyzer in line with an ISOPRIME 100 Isotopic Ratio Mass Spectrometer operating in continuous-flow mode. The system allows variations of the combustion module temperature up to 1050 °C useful for the extraction of different components having distinctive destabilization temperatures. C and N elemental concentrations were reported in weight percent (wt%). $^{13}C/^{12}C$, $^{15}N/^{14}N$ isotopic ratios (R) were expressed as $\delta(‰) = (1000*[R_{sample}-R_{standard}]/R_{standard})$, relative to the international isotope standards Pee Dee Belemnite (PDB) for carbon and AIR for nitrogen (Gonfiantini et al., 1995).

Powdered samples, introduced in tin capsules, were wrapped and weighed; these capsules, containing up to 40 mg of sample, were subsequently introduced in the Vario Micro Cube autosampler to be analysed. Flash combustion occurred in a sealed quartz tube filled with copper oxide (which acts as catalyst), in excess of high purity (grade 6.0) O_2 gas. Freed gaseous species were transferred in a reduction quartz tube (at 550 °C) filled with metallic copper wires to reduce the nitrogen oxides (NO_x) to N_2. The formed analyte gases, carried by He (grade 5.0) gas, passed through a water-trap filled with Sicapent to remove moisture. N_2 and CO_2 were separated by a temperature programmable desorption column (TPD) and quantitatively determined on a thermal-conductivity detector (TCD). Sample N_2 was transferred directly to the interfaced IRMS for isotopic composition determination, while CO_2 was held by the TPD column, kept at room temperatures 20–25 °C. When N_2 isotopic analysis was over, CO_2 was desorbed from the TPD column raising the temperature to 210 °C, finally reaching the IRMS for the determination of carbon isotopic ratios. The detection of the distinct isotopic masses of the sample was sandwiched between that of reference N_2 and CO_2 (5 grade purity) gases. Calibration was obtained using a series of reference materials, such as the limestone JLs-1 (Kusaka and Nakano, 2014), the peach leaves NIST SRM1547 (Dutta et al., 2006), the Carrara Marble (calibrated at the Institute of Geoscience and Georesources of the National Council of Researches of Pisa), and the synthetic sulfanilamide provided by Isoprime Ltd. Mass peaks were recalculated as isotopic ratios by the Ion Vantage software package. Reference and carrier gases of certified purity were provided by SIAD Ltd. Precision of elemental concentration measurement were estimated by repeated analyses of the standards, and accuracy estimated by the comparison between reference and measured values, were in the order of 5% of the absolute measured value. Uncertainties, increase for contents approaching the detection limit (0.001 wt %). The $\delta^{13}C$ and $\delta^{15}N$ values were characterised by an average standard deviation (1 sigma) of ± 0.1‰ and ± 0.3‰, respectively as defined by repeated analyses of the above mentioned standards.

3.3. Discrimination of soil inorganic and organic pools

Recent studies on the discrimination of carbon fractions in soils and sediments emphasised that acidification methods for carbonate removal can also lead to variable losses of organic carbon, potentially inducing significant deviations in the associated isotopic values (e.g., Serrano et al., 2008; Brodie et al., 2011 and the references therein; Schlacher and Connolly, 2014 and the references therein). On this basis, in this work the elemental and isotopic compositions of the of Total Carbon (TC), Organic Carbon (TOC), Inorganic Carbon (TIC) and the associated nitrogen fractions, were carried out according to the method proposed by Natali and Bianchini (2014; 2015), which was specifically refined for

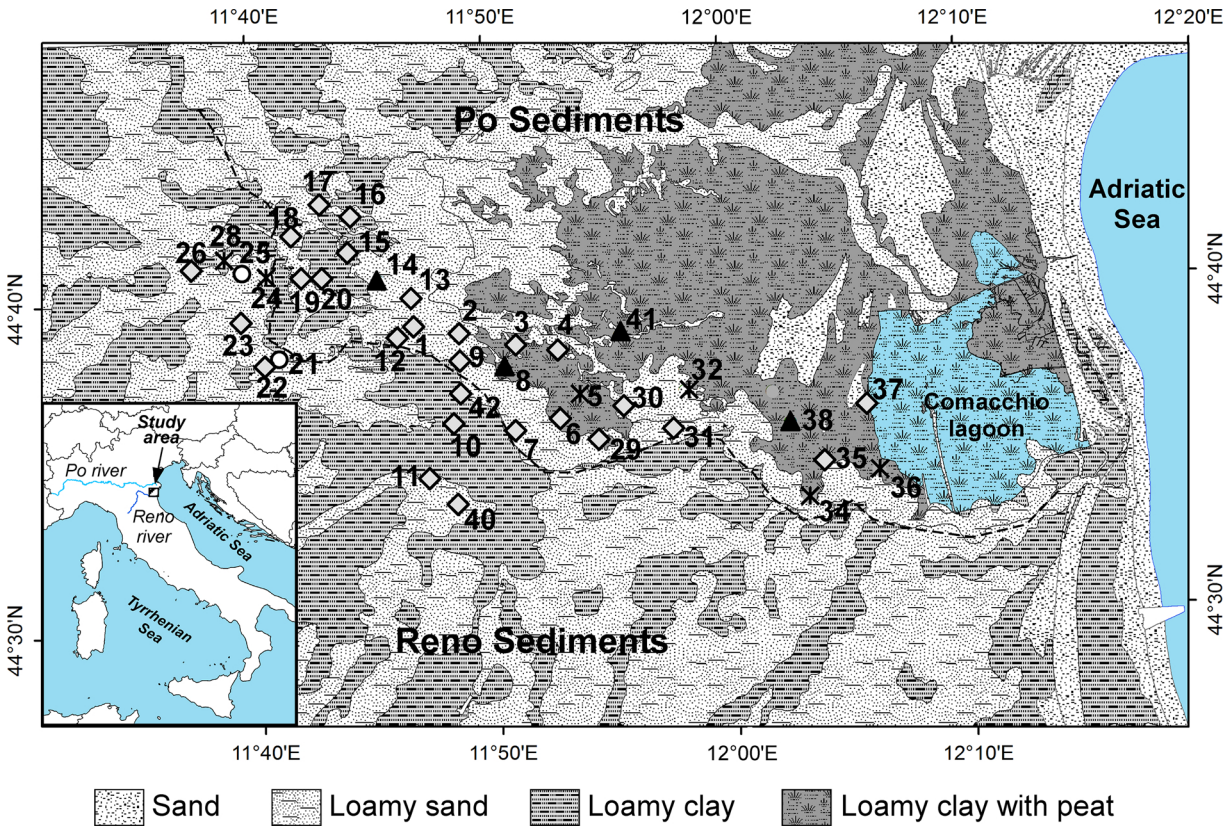

Fig. 1. Simplified sedimentological map of the investigated area which is located in the easternmost part of the Padanian plain between the Po and Reno riverine systems. Symbols refer to sample groups identified by cluster analysis and can be roughly ascribed to the related depositional environments. See chapter 4.1 for further details.

soil samples by Natali et al. (2018). According to this analytical protocol:

- TC (and TN) was carried out by EA-IRMS combusting at 950 °C the bulk sample;
- TOC was carried out by EA-IRMS combusting at 500 °C the bulk sample;
- TIC was carried out by EA-IRMS combusting at 950 °C the sample deprived of organic matter, i.e. preliminary burnt in a muffle furnace at 550 °C for 12 h; the relative gravimetric loss (LOI) was also determined in order to correct the elemental concentration of the TIC fraction.

The resulting wt% and $\delta^{13}C$ (‰) of the TOC and TIC fractions allowed a mass balance to calculate a theoretical TC fingerprint which was compared with that directly measured ($\delta^{13}C_{TC\ Measured}$):

$$\delta^{13}C_{TC\ Theoretical} = (\delta^{13}C_{TOC} * X_{TOC} + \delta^{13}C_{TIC} * X_{TIC})/(X_{TOC} + X_{TIC})$$

where X_{TOC} and X_{TIC} represent the organic and inorganic fractions, respectively.

The difference between theoretical and measured bulk isotopic ratios, expressed as $\Delta^{13}C$, complements the elemental carbon recovery and was used to cross-check the reliability of the method:

$$\Delta^{13}C = \delta^{13}C_{TC\ Measured} - \delta^{13}C_{TC\ Theoretical}$$

Summarising, in order to correctly measure the OC and IC fractions by thermal separation, we suggest combustion at 500 °C for the former, and thermal pre-treatment at 550 °C followed by combustion at 950 °C for the latter. This represents the best compromise that excludes the contribution of pedogenic minerals (oxalates/secondary metastable carbonates) to the OC, which are included in the IC fraction, together with the most thermally recalcitrant black carbon components (Natali et al., 2018). The latter are represented by subordinate mineralised carbon forms such as graphite, and by anthropogenic soot, which is abundant only in the contaminated soils of urban environments.

On a subset of 15 samples, the SOM was chemically separated in Non-Extractable Organic Matter (NEOM), Humic and Fulvic Acids (HA and FA, respectively) using a strongly chelating high pH solution according to Vittori Antisari et al. (2010). Briefly, 10 *g* of soil were placed in a 250 ml teflon bottle adding 100 ml of 0.1 M $Na_4P_2O_7$ plus 0.1 M NaOH solution and shaken in a Dubnoff water bath for 24 h at 65 °C. Afterwards, the samples were centrifuged at 7000 rpm for 20 min and the supernatant was separated from the mineral fraction. The extracted solution was filtered at 0.45 µm with Millipore vacuum filter. The total extracted solutions were acidified at pH value lower than 2 using 6 M HCl, in order to force the HA precipitation. After centrifugation at 8000 rpm for 20 min the HA were isolated, then re-dissolved with 0.5 M NaOH solution. This last step was repeated three times. The FA fraction was separated by no-humic compounds using solid chromatography techniques with polyvinilpirrolidone (PVP) following the procedures given in Ciavatta et al. (1990). The HA and FA fractions were purified using Spectra-por dialyzing membranes (MWCO 6000–8000 Da and 1000 Da, for HA and FA, respectively), and after dialysis the purified samples were freeze-dried and lyophilized.

4. Results

4.1. C and N elemental and isotopic soil composition

The total carbon (TC) and nitrogen (TN) elemental and isotopic analyses were carried out on 39 subsoil (*B*) samples at 100–120 cm depth in order to define the natural background and to characterise different depositional facies. The analyses, reported in Table 1,

Table 1
Carbon and Nitrogen elemental and isotopic composition and cluster analysis classification of soils from the Padanian deltaic area.

Sample	TN (wt%)	TC (wt%)	$\delta^{13}C_{TC}$ (‰)	$\delta^{15}N_{TN}$ (‰)	Cluster
90-110 cm depth					
1B	0.05	2.39	−5.0	–	L
2B	0.05	2.53	−5.3	1.6	L
3B	0.04	2.06	−4.0	2.9	L
4B	0.06	2.09	−6.6	–	L
5B	0.08	2.43	−11.2	−1.2	M
6B	0.06	2.91	−5.5	2.8	L
7B	0.04	2.91	−3.3	3.7	L
8B	0.08	0.89	−19.0	3.8	S
9B	0.05	2.09	−4.2	–	L
12B	0.06	2.71	−4.5	3.6	L
13B	0.08	1.78	−9.9	6.8	L
14B	0.11	1.12	−17.1	5.2	S
15B	0.05	2.21	−4.9	−0.7	L
16B	0.05	2.48	−4.4	1.8	L
17B	0.03	2.41	−4.0	–	L
18B	0.05	2.76	−4.2	1.6	L
19B	0.03	2.08	−5.0	2.9	L
20B	0.09	1.19	−17.2	7.1	S
29B	0.11	2.70	−10.0	4.7	M
30B	0.06	2.77	−4.7	2.4	L
31B	0.04	2.74	−5.1	–	L
32B	0.17	3.40	−12.3	3.4	M
34B	0.10	3.11	−7.4	4.7	M
35B	0.05	2.76	−3.5	0.3	L
36B	0.14	3.71	−12.2	3.3	M
37B	0.03	1.96	−3.5	–	L
38B	0.78	11.93	−28.2	1.6	S
41B	0.18	1.60	−25.2	3.0	S
10B	0.09	2.59	−7.4	2.5	L
11B	0.03	2.92	−2.9	1.8	L
21B	0.03	2.72	−2.5	3.0	P
22B	0.04	2.91	−4.2	–	L
23B	0.05	2.90	−4.8	1.8	L
24B	0.10	2.21	−9.8	3.8	M
25B	0.01	3.03	−1.2	–	P
26B	0.06	2.45	−5.6	3.2	L
28B	0.18	2.89	−13.3	3.1	M
40B	0.04	2.80	−3.1	2.0	L
42B	0.06	2.33	−5.4	2.4	L
20-30 cm depth					
6A	0.22	4.37	−13.7	4.1	
8A	0.19	2.84	−14.1	8.2	
16 A	0.16	1.31	−21.9	4.9	
23A	0.16	3.37	−10.8	5.2	
26A	0.15	2.85	−9.7	5.0	
19A	0.16	2.29	−15.2	7.6	
30A	0.14	3.56	−10.1	4.9	
32A	0.11	3.20	−8.6	4.3	
34A	0.15	3.27	−10.4	4.5	
38A	0.45	6.49	−23.1	3.4	
41A	0.28	3.27	−19.2	10.0	

highlight that subsoils are characterised by a wide elemental and isotopic compositional variability. In particular, TC ranges from 0.89 wt% (8B) to 11.93 wt% (38B) and TN from 0.01 wt% (25B) to 0.78 wt% (38B). The isotopic composition of the investigated subsoils showed $\delta^{13}C_{TC}$ values varying from −28.2‰ (38B) to −1.2‰ (25B) whereas the $\delta^{15}N$ values range between -0.7‰ (15B) and 6.8‰ (13B). Bivariate statistical analysis based on Pearson correlation shows that TN is negatively correlated with $\delta^{13}C_{TC}$ value (r = −0.84) whereas no other significant correlation among these variables have been observed.

These C and N data have been also compared with the major and trace elements (obtained by XRF) reported for the same samples by Di Giuseppe et al. (2014d) and the resulting correlation matrix highlight that TC is positively correlated with CaO (r = 0.73) and to a lesser extent with Sr (r = 0.66), suggesting a significant presence of carbonates in these soils. This is confirmed by the significant ($p < 0.05$) negative correlation of TC with other elements typically contained in silicates (e.g. Pb r = −0.73, Rb r = −0.71 and Th r = −0.70) as well as by the parallel positive correlation of $\delta^{13}C$ with CaO (r = 0.75) and Sr (r = 0.73). Moreover, the carbon isotopic ratio displays a well-defined negative correlation with Al_2O_3 (r = −0.73), K_2O (r = −0.74), Pb (r = −0.71), Cu (r = −0.74), and to a lesser extent with Rb (r = −0.69), V (r = −0.67), Zn (r = −0.68) and Th (r = −0.62) which are all elements typically contained in phyllosilicates and/or bound to organic matter that is generally predominant in the soil fine fractions.

A hierarchical cluster analysis has been carried out combining the new data (TC, TN, $\delta^{13}C_{TC}$) with the pre-existing XRF analyses (Di Giuseppe et al., 2014d). The results suggest that the sample population can be subdivided in 4 groups that broadly conform to the distinct depositional facies highlighted by Di Giuseppe et al., 2014a (P – paleochannels, L – levees, M – marshes, S – swamps).

The soils grouped by P cluster are characterised by shallow water table, formed in alluvium and receive high moisture (e.g. Udifluventic Haplustepts and Oxyaquic Ustifluvents); they are characterised by the following averaged values: C = 2.88 wt%, N = 0.02 wt%, $\delta^{13}C_{TC}$ = −1.8‰, $\delta^{15}N$ = 3.0‰.

The soils grouped by L cluster are formed under redox depletion with low chroma commonly in a brownish or reddish matrix in the subsoil (Aquic Haplustepts); they are characterised by the following averaged values: C = 2.50 wt%, N = 0.05 wt%, $\delta^{13}C_{TC}$ = −4.8‰, $\delta^{15}N$ = 2.4‰.

The samples grouped in the cluster M are soils typically derived from coastal marshes in riverine deltas (e.g. Terric Sulfisaprists and Sulfic Endoaquepts); they are characterised by the following averaged values: C = 2.91 wt%, N = 0.13 wt%, $\delta^{13}C_{TC}$ = −10.9‰, $\delta^{15}N$ = 3.1‰.

The samples grouped in the cluster S are soils characterised by silty clay textured alluvium deposit, formed in internal deltaic sectors of the Po riverine system (Aquic Calciusteps, Sulfic Endoaquepts); they are characterised by the following averaged values: C = 3.34 wt%, N = 0.11 wt%, $\delta^{13}C_{TC}$ = −21.3‰ $\delta^{15}N$ = 4.2‰. We included in this group the unclusterized sample 38 (Fluvaquentic Endoaquolls), showing an extreme C and N content (TC = 11.93 wt%, N = 0.78 wt%) coupled with very ^{13}C and ^{15}N depleted isotopic composition ($\delta^{13}C_{TC}$ = −28.2‰, $\delta^{15}N$ = 1.6‰).

Coherently, the compositional variation of the identified sample groups in terms of TC, N, and $\delta^{13}C_{TC}$ is reported in Fig. 2. These clusters obtained elaborating chemical and isotopic data, roughly discriminate distinct textural groups, as evidenced by the Sand-Silt-Clay ternary diagram of Supplementary Fig. 1.

The new data potentially provide constraints on the carbon and nitrogen pools of the investigated soils. In particular, the distribution of TC, $\delta^{13}C_{TC}$ vs CaO and Sr/Rb are useful to identify the main mineral and organic components that induce the observed variation (Fig. 3). In Fig. 3a (CaO vs TC), some samples straddle along calcite stoichiometric line (clusters L) suggesting that carbonate represents the main C pool. Other samples plot on the right of the calcite stoichiometric line (clusters M and S) because they contain a significant amount of OM and/or authigenic minerals such as oxalate. Only few samples plot on the left of the calcite stoichiometric line suggesting a variable contribution by CaO-bearing silicate minerals such as feldspars (cluster P). In Fig. 3b (CaO vs $\delta^{13}C_{TC}$), most samples are distributed along the mixing line between primary carbonates (typically characterised by CaO 12 wt% and $\delta^{13}C_{TC}$ approaching 0‰) and CaO-free OM that conforms to C3 photosynthetic pathway vegetation ($\delta^{13}C$ ca. −27‰, DeNiro and Epstein, 1978). However, some samples (cluster M) deviate from this hyperbolic mixing trend suggesting the presence of a further CaO-bearing end-member characterised by ^{13}C depleted isotopic composition, possibly consisting of oxalate or authigenic carbonate and/or sulphates (Dauer and Perakis, 2014; Kovda et al., 2014). Fig. 3c, reporting Sr/Rb vs $\delta^{13}C_{TC}$, confirms that most of the samples can be interpreted as mixing of OM-free coarse sediments and OM-rich fine sediments. However, even in this case some samples (cluster M) are

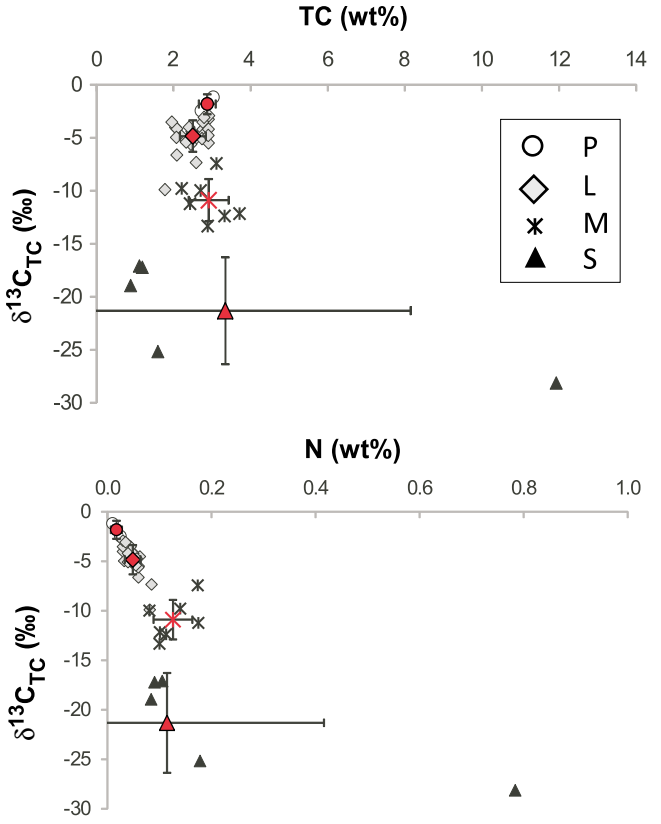

Fig. 2. Total Carbon (TC) and nitrogen (N) versus TC isotope ratio ($\delta^{13}C_{TC}$) of subsoils from the easternmost Padanian plain. Symbols refer to sample groups identified by cluster analysis and can be roughly ascribed to the related depositional environments. Red symbols represent average values for each cluster with the related standard deviation. See chapter 4.1 for further details (For interpretation of the references to colour in this figure legend, the reader is referred to the web version of this article).

displaced from this trend suggesting the presence of a third end-member possibly consisting of oxalates and authigenic carbonates and/or sulphates.

A subset of 11 superficial (*A*) soils representative of the plough horizon (20–30 cm depth) have been also analysed and the results have been compared with their respective *B* subsoils with the aim of delineate the carbon and nitrogen variability, and to emphasise the possible existence of Top Enrichment Factors (TEF). This parameter is calculated as the ratio between topsoil and subsoil concentrations (Ungaro et al., 2008), and could be related to anthropogenic activities. The elemental analyses reveal that the average TC content of the sampled soils is slightly higher in the *A* horizon (3.35 wt%) than in the and the *B* layer (2.73 wt%), although extreme compositions exist at both depths (SD of 1.29 and 2.94, respectively). Accordingly, the average TEF is 1.3 possibly reflecting the presence of OM derived from both crop residua or organic fertilizers (e.g., manure or slurry) re-incorporated in the soil by tillage. The total carbon isotopic composition is decidedly more negative in the *A* (average $\delta^{13}C_{TC}$ −14.3‰) with respect to the relative *B* (average $\delta^{13}C_{TC}$ -8.3‰) samples, with the exception of two *B* samples characterised by ^{13}C-depleted composition (38B $\delta^{13}C_{TC}$ -28.2‰; 41B $\delta^{13}C_{TC}$ −25.2‰) in relation to their peculiar pedological characters (Fluvaquentic Endoaquolls and Sulfic Endoaquepts, respectively).

Coherently, the total nitrogen elemental content (TN) is higher in the *A* (average 0.20 wt%) with respect to *B* (average 0.09 wt%) samples, which implies an average TEF of 2.4. The associated nitrogen isotopic composition shows average $\delta^{15}N$ of 5.7‰ in *A* and of 2.9‰ in *B* samples. Noteworthy, the TN negatively correlates with $\delta^{13}C_{TC}$ and

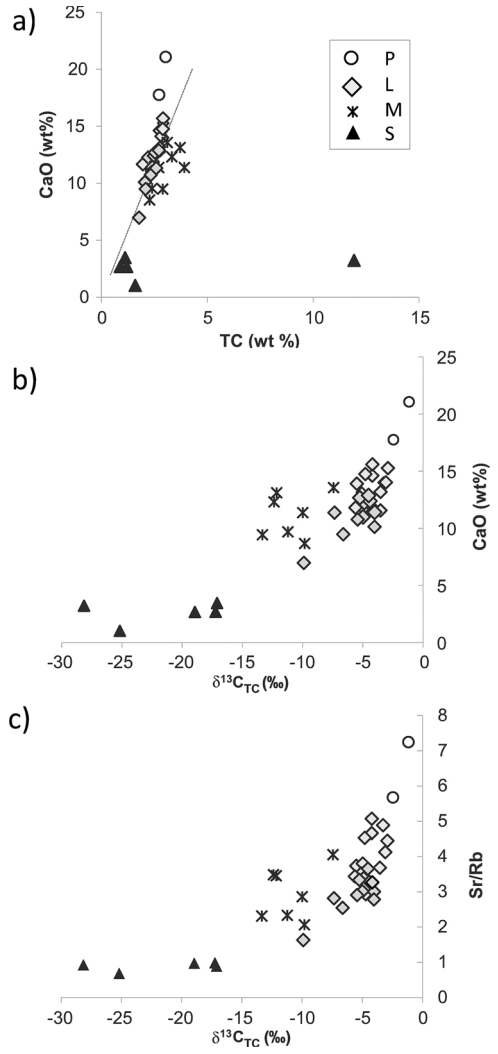

Fig. 3. Distribution of (a) TC vs CaO, (b) $\delta^{13}C_{TC}$ vs CaO and (c) $\delta^{13}C_{TC}$ vs Sr/Rb of the investigated soils grouped in different clusters; dashed line in (a) represents the calcite stoichiometric line.

the highest TN content (0.78 wt%) is detected in the above mentioned sample 38B.

4.2. Organic vs inorganic carbon pools

The elemental and isotopic TOC and TIC determinations have been carried out on 20 samples (13 *B* subsoils and 11 *A* topsoils), representative of the different depositional facies delineated above. The results are reported in Table 2, which also includes the calculated elemental and isotopic carbon recoveries, and in Fig. 4. TOC average is 1.8 wt% in *A* samples and 0.6 wt% in *B* samples, which corresponds to a TOC fraction (TOC/TC*100) of ca. 52% of the TC in the *A* samples that is decidedly higher than that recorded in *B* samples (TOC ca. 35% of the TC). The average TOC isotopic composition ($\delta^{13}C_{TOC}$) of the *A* topsoils is -24.8‰, showing a $\delta^{13}C$ depletion of ca. 2.5‰ with respect to that associated with *B* subsoils (average $\delta^{13}C_{TOC}$ = -22.3‰). A notable exception is represented by the two samples 41B and 38B in which TOC is nearly 90% of the TC, and characterised by comparatively more negative $\delta^{13}C_{TOC}$ values (-26.0 and -27.9‰, respectively).

The average TIC is similar in the *A* (1.7 wt%, SD = 0.8) and *B* (1.9 wt%, SD = 0.8) samples, but it represents different proportion with respect to the TC (TIC/TC*100). Average TIC fraction is lower in the *A* (ca. 48% of the TC) with respect to that of the *B* samples where it is ca. 65% of the TC; in organic-rich samples 41B and 38B TIC accounts for

Table 2
Carbon elemental and isotopic speciation of organic and inorganic carbon pools from selected superficial and deep soils.

		Measured TC		TIC		TOC		Recovery (TC-TIC + TOC)			
Sample	LOI	C (wt%)	$\delta^{13}C_{TC}$ (‰)	C (wt%)	$\delta^{13}C_{TIC}$ (‰)	C (wt%)	$\delta^{13}C_{TOC}$ (‰)	C (%)	$\Delta^{13}C$ (‰)	$\Delta^{13}C_{TIC\text{-}TOC}$ (‰)	Cluster
90-110 cm depth											
21B	2.31	2.72	−2.5	2.44	−0.6	0.22	−23.4	98	0.0	*−22.8*	P
											P
25B	1.36	3.03	−1.2	2.83	−0.5	0.13	−20.9	98	0.2	*−20.4*	P
6B	6.54	2.91	−5.5	2.39	−2.0	0.47	−23.3	98	0.0	*−21.3*	L
16B	5.30	2.48	−5.2	2.09	−2.2	0.4	−21.9	101	0.2	*−19.7*	L
19B	3.52	2.08	−5.0	1.76	−2.3	0.34	−22.2	101	0.6	*−19.9*	L
23B	4.39	2.90	−4.8	2.48	−1.8	0.45	−21.6	101	0.1	*−19.8*	L
26B	4.61	2.45	−5.6	1.98	−1.5	0.46	−22.6	100	−0.1	*−21.1*	L
30B	5.08	2.77	−4.7	2.33	−1.8	0.40	−21.9	99	0.0	*−20.2*	L
32B	9.71	3.40	−12.3	1.49	−1.2	1.97	−20.9	102	0.1	*−18.6*	M
34B	7.59	3.11	−7.4	2.23	−1.9	0.82	−21.5	98	−0.2	*−17.2*	M
8B	9.19	0.89	−19.0	0.28	−8.8	0.61	−24.4	100	0.6	*−15.6*	S
38B	30.10	11.9	−28.2	0.03	−19.4	11.7	−28.7	98	0.5	*−9.3*	S
41B	9.95	1.60	−25.2	0.06	−10.8	1.52	−25.0	99	−0.7	*−11.3*	S
20-30 cm depth											
6A	9.29	4.37	−13.7	2.18	−2.9	2.15	−25.1	99	0.2	*−21.7*	
16 A	10.74	1.31	−21.9	0.11	−6.7	1.22	−22.8	102	−0.4	*−12.9*	
19A	6.82	2.29	−15.2	1.04	−3.6	1.26	−24.6	100	−0.1	*−20.6*	
23A	6.11	3.37	−10.8	2.17	−2.0	1.25	−24.8	101	−0.4	*−22.8*	
26A	6.69	2.85	−9.7	1.84	−1.6	1.02	−24.4	100	0.0	*−22.8*	
30A	5.48	3.56	−10.1	2.32	−1.5	1.21	−25.5	99	−0.3	*−24.1*	
32A	5.01	3.20	−8.6	2.28	−1.9	0.88	−24.6	99	−0.4	*−22.8*	
34A	4.25	3.27	−10.4	2.02	−1.1	1.22	−25.7	99	0.0	*−24.4*	
8A	7.76	2.72	−14.1	1.38	−3.5	1.32	−23.8	99	−0.6	*−20.3*	
38A	5.67	6.49	−23.1	0.94	−3.4	5.47	−25.9	99	−0.5	*−24.4*	
41A	14.8	3.27	−19.2	0.95	−6.0	2.28	−24.5	99	−0.1	*−23.4*	

5.0% and 0.2%, respectively. The average TIC isotopic composition ($\delta^{13}C_{TIC}$) is slightly enriched in ^{13}C in the *A* topsoils ($\delta^{13}C_{TIC}$ = -3.1‰, SD = 1.8) with respect to that recorded in the *B* undisturbed layer ($\delta^{13}C_{TIC}$ = -4.2‰, SD = 5.5). Some decidedly negative isotopic values are observed in the topsoil 16 A ($\delta^{13}C_{TIC}$ = -6.7‰) and in the subsoils of the S group ($\delta^{13}C_{TIC}$ from -8.8 to -19.4‰), plausibly resulting from the presence of authigenic minerals (oxalate and/or carbonates; Millière et al., 2011; Lawrence et al., 2015; Zamanian et al., 2016), or from the existence of thermally recalcitrant OM compounds (Johnson et al., 2015).

As concerns the variation of the soil carbon pools in different depositional facies (defined only for subsoils), the TOC fraction respect to the TC increases from P (average of 6%), to L and M (average of 16% and 42%, respectively), reaching extreme values in S samples (average of 87%). The associated isotopic composition ($\delta^{13}C_{TOC}$) ranges around -22‰ in L and M samples, and becomes decidedly more negative in S samples (average of -26.1‰). Analogies are observed in the isotopic composition of the TIC fraction that is comparable in L and M samples ($\delta^{13}C_{TIC}$ around -1.8‰) and becomes decidedly more negative in the S samples (average $\delta^{13}C_{TIC}$ -13‰).

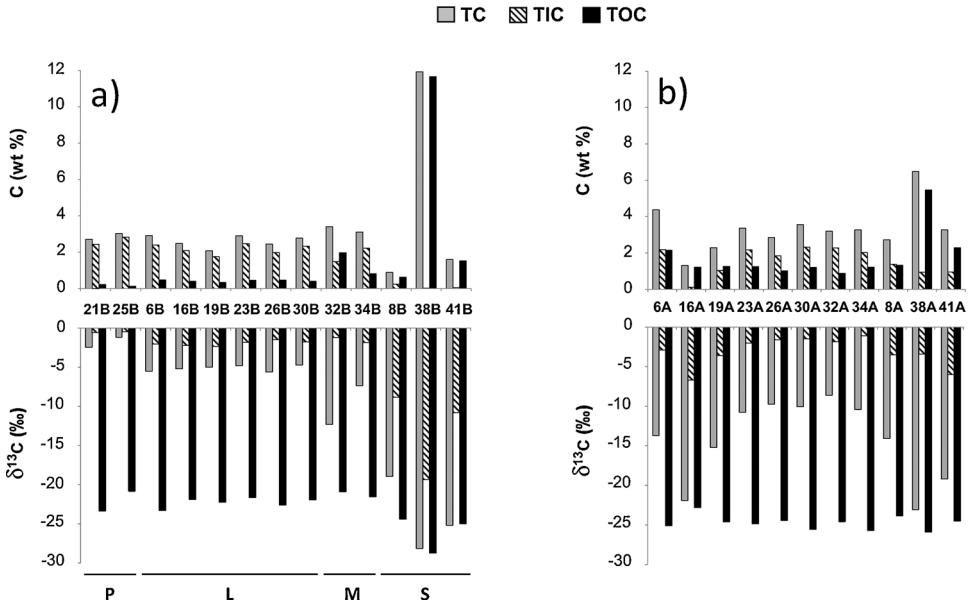

Fig. 4. Carbon elemental and isotopic composition of the different carbon fraction (TC, TIC and TOC) in *A* and *B* soils from the Padanian plain. For the *B* soils the membership to the relative cluster is indicated.

Table 3
Carbon and nitrogen elemental and isotopic composition of organic carbon pools from selected superficial and deep soils.

Sample	*Organic Matter* NEOM C (wt%)	$\delta^{13}C$ (‰)	HA C (wt%)	$\delta^{13}C$ (‰)	N (wt%)	$\delta^{15}N$ (‰)	FA C (wt%)	$\delta^{13}C$ (‰)	N (wt%)	$\delta^{15}N$ (‰)	Cluster
100-120 cm depth											
6B	0.36	−18.5	36.4	−25.3	3.02	3.6	46.8	−26.1	4.11	0.6	L
19B	0.15	−16.3	–	–	–	–	38.2	−26.7	3.41	4.5	L
26B	0.46	−21.0	41.8	−26.6	3.29	4.5	37.4	−25.9	2.84	0.7	L
30B	0.32	−17.6	41.3	−25.1	3.13	4.7	28.0	−25.4	1.60	1.7	L
32B	0.66	−21.6	42.8	−25.0	3.34	3.3	35.9	−24.7	2.41	2.2	M
34B	0.45	−18.3	33.6	−24.7	3.11	5.3	39.8	−25.2	3.03	2.2	M
38B	4.83	−28.6	37.1	−27.0	2.62	1.0	36.7	−27.4	1.59	1.1	S
41B	1.08	−24.3	42.1	−25.9	3.36	1.3	38.0	−25.9	2.83	1.0	S
20-30 cm depth											
6A	0.88	−22.1	37.6	−26.1	3.15	5.9	33.8	−26.3	2.25	2.5	
8A	0.67	−20.8	30.3	−24.6	2.91	9.7	38.2	−25.3	3.15	5.7	
16 A	0.47	−20.5	27.5	−24.7	2.37	5.5	36.0	−25.3	3.20	1.6	
19A	0.41	−19.2	40.7	−25.4	3.74	5.8	38.8	−26.0	2.96	4.7	
30A	0.55	−21.2	42.5	−26.4	3.42	5.2	36.9	−27.0	2.77	0.6	
32A	0.42	−19.2	42.2	−24.9	3.98	6.3	36.6	−26.2	2.62	3.3	
34A	0.65	−22.4	42.1	−26.9	4.11	5.4	39.8	−27.5	3.03	2.2	

4.3. Carbon (and nitrogen) speciation of organic matter

The SOM characterisation has been carried out on a subset of 15 samples (8 from the *B* and 7 from the *A* horizons) by carbon isotopic analyses of the chemically non-extractable organic matter (NEOM) and of extracted fulvic (FA) and humic acids (HA, Table 3 and Fig. 5). The carbon isotopic composition of NEOM in *B* samples is generally more ^{13}C-enriched (average of -18.9‰) than that of *A* samples (average of -20.8‰), with the exception of the organic-rich samples 38B ($\delta^{13}C_{NEOM}$ = −28.6‰) and 41B ($\delta^{13}C_{NEOM}$ = −24.3‰).

The carbon isotopic composition of extractable OM pools (EOM) is rather homogeneous in soils both from the *B* and *A* horizons. In particular, FA show an average $\delta^{13}C_{FA}$ of −25.9‰ (SD = 0.9‰) and of −26.2‰ (SD = 0.8‰) for the *B* and *A* samples, respectively. These values are slightly ^{13}C-depleted in comparison with those obtained for HA which show average $\delta^{13}C_{HA}$ of -25.7‰ (SD = 0.9‰) in the *B* soils and of −25.6‰ (SD = 0.9‰) in *A* soils. On the whole, the nitrogen isotopic composition shows distinctly higher values in HA (average of $\delta^{15}N_{HA}$ = 4.8‰) respect to that recorded in FA (average of $\delta^{15}N_{FA}$ = 2.3‰). The nitrogen isotopic composition of both the extractable OM pools also exhibits a marked ^{15}N depletion with depth (Fig. 6). In particular, averaged $\delta^{15}N$ values in HA decrease from 6.3‰ (SD = 1.5‰) in *A* samples to 3.4‰ (SD = 0.8‰) in *B* samples, whereas FA show a less marked variation ($\delta^{15}N_{FA}$ = 2.9‰, SD = 1.8‰ for *A* soils and $\delta^{15}N$ = 1.8‰, SD = 1.4‰ for *B* soils).

Noteworthy, there are differences in the carbon isotopic composition of SOM pools in samples pertaining to distinct depositional facies. The $\delta^{13}C_{NEOM}$ generally shows the less negative values in L samples (up to −16.3‰ in 19B), a tendency toward more negative values in M samples (average of −20.0‰), and the more ^{13}C-depleted values in S samples (down to −28.6‰ in 38B). The differences in terms of carbon isotopic composition of SOM extractable pools ($\delta^{13}C_{EOM}$) among the distinct soil groups are less marked, although the S sample 38B is invariably characterised by the more negative $\delta^{13}C$ values (down to −27.0‰ in HA, −27.4‰ in FA).

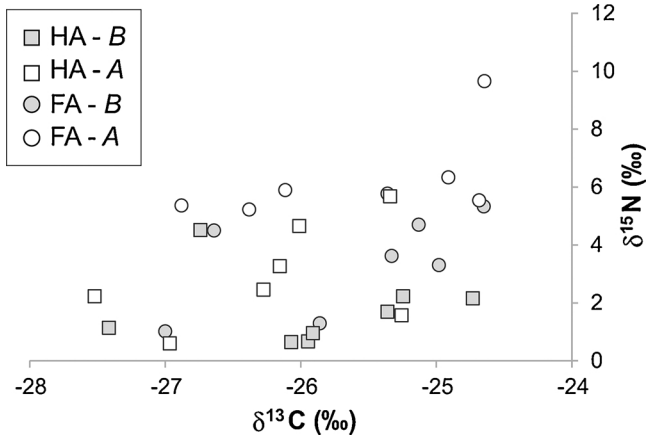

Fig. 6. C and N isotopic composition of humic and fulvic acids extracted from the investigated *A* and *B* soils. For the *B* soils the membership to the relative cluster is indicated.

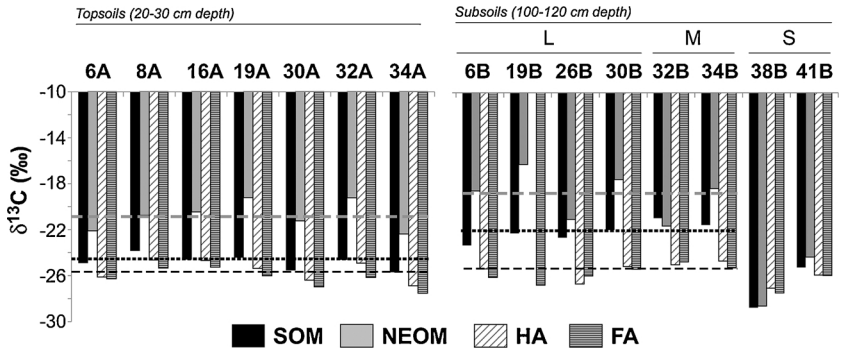

Fig. 5. $\delta^{13}C$ (‰) histograms showing the compositions of bulk SOM (expressed by $\delta^{13}C_{TOC}$) and relative non-extractable (NEOM) and extractable (EOM, HA and FA) fractions of selected *A* and *B* soils from the easternmost Padanian plain. For the *B* soils the membership to the relative cluster is indicated. The averaged isotopic values for SOM (dotted black line), EOM (dashed black line) and NEOM (dashed gray line) are also reported.

5. Discussion

5.1. Insights from the inorganic carbon fraction

The elemental and isotopic carbon speciation of the studied soils allows to investigate the nature of the carbonatic fraction included the Padanian alluvial plain sediments. From one hand, where organic matter is subordinate, the isotopic fingerprint of the TIC maintains reliable information on the composition of primary carbonate mother rocks, allowing a possible distinction among different sources and provenance. From another hand, where organic matter become prevalent, the carbon isotopic fingerprint of the TIC allows to check the involvement of organic matter in biomineralization processes and/or formation of secondary pedogenic carbonates.

The inorganic carbon fraction and the associated isotopic composition of the investigated soils show a bimodal distribution: most of the samples show a narrow range of ^{13}C-enriched isotopic composition ($\delta^{13}C_{TIC}$ from −1.5 to −4.2‰) which is associated with a broad TIC fraction (TIC/TC*100) varying in the range 45–85% of the TC, whereas TOC-rich samples (70–98% of the TC, generally ascribed to the S group) are characterised by a distinctly negative $\delta^{13}C_{TIC}$ range (from −8.8 to −19.4‰). The predominant group shows a TIC isotopic composition which is compatible with that of sedimentary marine carbonates supplied by the drainage network during the development and progradation of the alluvial plain, whereas the subordinate group -including samples 8B, 38B, 41B and 16 A- shows $\delta^{13}C_{TIC}$ values similar to that recorded in palustrine carbonates developed in a swampy environment (Alonso-Zarza et al., 2006; Dunagan and Turner, 2004). In the relative soils dynamics are particularly complex due to cyclic waterlogged and drained conditions, implying variable interaction of carbonates with the organic matter, as reflected by the difference obtained by the respective isotopic ratios ($\Delta^{13}C_{TIC\text{-}TOC}$), which range from -9.3 to -15.6‰ (Table 2). Therefore, the TIC isotopic composition of these samples, can be considered a proxy of a peculiar low-energy depositional environment typical of the reclaimed wetlands. An additional hypothesis deals with the neo-formation of carbonate from fluids containing ^{13}C-depleted dissolved inorganic carbon ($\delta^{13}C_{DIC}$ down to -40‰), such as those observed in the local aquifers by Caschetto et al. (2017).

5.2. Insights from the organic pools

The SOM content is generally more abundant in *A* samples with respect to the deeper *B* samples. However, the more negative bulk $\delta^{13}C_{TC}$ of *A* topsoils respect to *B* subsoils, cannot be simply ascribed to a higher SOM content. In fact, in the investigated soils more negative SOM carbon isotopic ratios are characteristic of *A* samples (average $\delta^{13}C_{TOC}$ -24.7‰) with respect to *B* samples (average $\delta^{13}C_{TOC}$ -22.0‰), with the exception of the S samples showing the most negative ($\delta^{13}C_{TOC}$ from -24.4 to -28.7‰). According to De Clercq et al. (2015), this suggests a lower SOM maturity at the surface.

The NEOM carbon isotopic ratio is more ^{13}C-enriched in *B* samples ($\delta^{13}C_{NEOM}$ -18.9‰ on average) with respect to *A* samples ($\delta^{13}C_{NEOM}$ -20.8‰ on average) probably due to multiple biologically-driven reactions producing fugitive isotopic light compounds, and leaving a ^{13}C-enriched residual OM (Rumpel and Kögel-Knabner, 2010).

HA and FA are both strongly ^{13}C-depleted and don't display significant variation with depth. It is noteworthy that FA are generally characterised by slightly ^{13}C-depleted carbon isotopic ratios with respect to HA (average $\delta^{13}C$ -25.6‰ and -26.1‰, respectively) suggesting that they represent the extreme stage of SOM evolution, as also suggested by other studies (Agnelli et al., 2014).

In general, we observe a higher "absolute" C isotopic difference ($\Delta^{13}C_{NEOM\text{-}EOM}$) between non-extractable and extractable organic matter in *B* (average of -6.7‰) with respect to *A* (average of -5.1‰) soils, with the exception of samples belonging to the S group that are characterised by the lowest $\Delta^{13}C_{NEOM\text{-}EOM}$ (38B + 1.4‰, 41B -1.6‰). This suggests that *B* soils underwent a higher biogeochemical processing, whereas *A* soils are fed by "fresh" OM still unaffected by microbial reworking (De Clercq et al., 2015). The paucity of fractionation observed in the OM compounds of the two S subsoils plausibly reflects their Aquic and Sulfic character, which precludes high rate of microbial activity.

The carbon isotopic differences observed among HA and FA, are remarked by nitrogen isotopic ratios, that are more ^{15}N enriched in HA with respect to FA (average $\delta^{15}N$ 4.8‰ and 2.3‰, respectively). This fractionation should be associated to biogeochemical processes leading to their intrinsic formation or by a higher attitude of FA to exchange/incorporate synthetic nitrogen derived by inorganic fertilization with respect to HA (Stevenson and Cole, 1999). The systematic ^{15}N-depletion of nitrogen isotopic ratios of HA and FA in deep (average $\delta^{15}N$ 3.4‰ and 1.8‰, respectively) with respect to superficial (average $\delta^{15}N$ 6.3‰ and 2.9‰, respectively) samples, reflects the downward migration of inorganic compounds employed as fertilizers ($\delta^{15}N$ ca. 0). This is coherent with other studies of the same agricultural area, which emphasised the progressive leaching and percolation of N compounds along the soil profile (Colombani et al., 2011; Caschetto et al., 2017).

The current conditions of SOM in the investigated soils is summarized in Fig. 7, which reports the averaged compositions of bulk OM and of the related non-extractable and extractable fractions. In general, the study emphasises that, although the SOM is quantitatively more abundant in the superficial horizon, its stability is lower than that from deeper horizon. In particular, labile and isotopically lighter organic compounds tend to concentrate at the surface, probably as a result of combined mechanical and agro-chemical effects.

On the whole, the isotopic composition of SOM pools seems to be correlated with the pedological characters, which in turn reflect the depositional facies and the post-sedimentary evolution, which also includes anthropogenic activities. The SOM dynamics is expressed as a

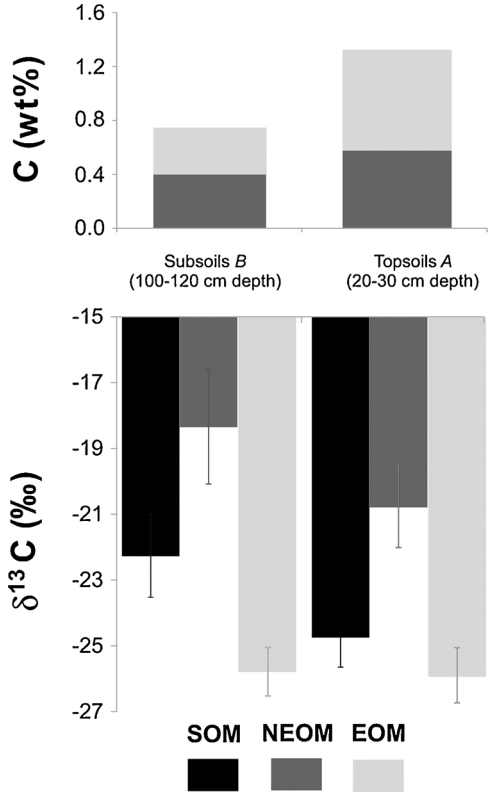

Fig. 7. $\delta^{13}C$ (‰) histograms showing the averaged compositions of bulk SOM (expressed by $\delta^{13}C_{TOC}$) and relative non-extractable (NEOM) and extractable (EOM = HA + FA) fractions of selected *A* and *B* soils from the easternmost Padanian plain. Bars represent standard deviations.

Table 4
TOC (%) in current day superficial soils compared to that reported in 1938 in samples from the same localities. Comparison is possible only for few sites where the georeferenced locations are coincident.

Sample	TOC (%)		ΔTOC_{70y}
	2012	1938	
6A	49	50	−1
23A	37	56	−19
26A	36	58	−22
32A	28	57	−30
34A	37	46	−9
8A	49	63	−14
38A	84	92	−8
41A	70	81	−11

Note: TOC (%) = TOC/TC (wt%) *100.

function of the isotope composition of the different carbon pools such as NEOM, HA and FA. The isotopic decoupling between NEOM and HA−FA (expressed by $\Delta^{13}C_{NEOM\text{-}EOM}$ ‰) is very similar in *A* samples (average of -5.1‰, SD = 1.0‰), whereas shows a marked variation in *B* samples (average of -6.7‰, SD = 3.8‰), reflecting the more complex evolutionary conditions of deep soil horizons, with respect to the plough horizon. In particular, in *B* soils, $\Delta^{13}C_{NEOM\text{-}EOM}$ display a significant positive correlation (r^2 = 0.83) with the TOC (%, calculated as TOC/TC*100), suggesting that soil samples having TOC higher than 90% undergone minimum SOM transformation and evolution ($\Delta^{13}C_{NEOM\text{-}EOM}$ around 0‰). This is the case of the TOC-rich samples of the S group, that although very different in terms of geochemical and grain size compositions, show similar hydromorphic pedological features (Aquic to Sulfic) that prevent SOM processing and evolution.

The SOC variation along the soil profile in the different depositional facies has been estimated by the difference of organic carbon percentages (TOC/TC*100) in *A* soils with respect to that in *B* subsoils. It can be systematically observed that TOC% at surface increases in L samples (20–77 %) and decreases in S samples (from -13 to -25%), whereas intermediate and more variable conditions characterise M samples. This implies that, in spite of the agricultural activities that add organic matter, S soils are affected by TOC losses at surface, which can be mainly attributed to oxidation induced by intensive agricultural practices. On the other hand, L soils can be affected by TOC losses at depth due to microbial degradation of SOM, which ultimately led to the observed ^{13}C-enriched isotopic composition (e.g.,Wynn et al., 2006).

Carbon losses can be estimated also by comparison with historical data that have been retrieved for a subset of sampling sites from an agronomic archive available at the Department of Agricultural and Food Sciences of the University of Bologna, including soil analyses carried out before war world two. This comparison highlights that the organic carbon fraction has been reduced at all sites, recording losses up to 30% over the last 70 years (Table 4).

Particular attention has to be paid to the peaty deposits that show distinctive features, diverging from most of the other samples and indicating peculiar SOM evolutionary processes; their SOM decomposition, with relative CO_2 emission in atmosphere, is potentially enhanced by wetland reclamation and agricultural activities that led to highly oxidative conditions (Hooijer et al., 2010). The related soil profile shows depletion of organic matter content toward the surface and temporal loss of the organic carbon fraction, estimated as 10–15% during the last 70 years (Table 4).

6. Conclusions

This paper implements previous geochemical studies of alluvial soils from the easternmost part of the Padanian plain (Northern Italy) within the Po river deltaic system. The new C-N elemental and isotopic data refine previous inferences on the depositional facies, on pedogenetic processes, as well as on anthropogenic influences. Noteworthy, C and N are fundamental elements invariably associated to the SOM and their budget is labile and less stable than that of lithophile elements. Results highlight that the followed approach is useful in the discrimination of the different carbon pools, in particular allowing SOM benchmark of the distinct depositional facies (in subsoils), and to evaluate the effect of agricultural activity on its evolution (in topsoils). Our results indicate that SOM of subsoils is generally affected by microbial degradation, with the exception of clayey and peaty deposits that represent a carbon reservoir in which biological activity is inhibited and SOM appears relatively preserved. However, the potential greenhouse gas contribution of the clayey and peaty soils is highlighted by the loss of organic fraction along the soil profiles, which account for ca. 20% of the original budget, plausibly in response to intense agricultural activities. More in general, on the basis of a comparison with historical data, we recorded variable (up to 30%) but ubiquitous losses of the organic fraction throughout the investigated area, over the last 70 years. Global warming can magnify the SOM deterioration (Oertel et al., 2016), and therefore reiteration of similar studies will be useful to monitor the SOM resilience, and to provide indications for sustainable agronomical approaches. The data recorded by this study therefore represent a snapshot of the current local conditions, useful to create a soil geochemical archive as a tool for monitoring natural (climatic) and anthropogenic variations. Furthermore, the obtained results could be relevant not only at the local scale but, more in general, for similar deltaic areas in temperate climate settings.

Acknowledgements

This study was supported by the European Agricultural Fund for Rural Development (project SaveSOC2, ID: 2017IT06RDEI5015638 v1), allocated by the Emilia-Romagna region (PSR 2014-2020). The authors gratefully acknowledge the two anonymous reviewer and the editor for their constructive comments, which helped to improve the earlier version of the manuscript.

Appendix A. Supplementary data

Supplementary material related to this article can be found, in the online version, at doi:https://doi.org/10.1016/j.chemer.2018.09.001.

References

Agnelli, A., Bol, R., Trumbore, S.E., Dixon, L., Cocco, S., Corti, G., 2014. Carbon and nitrogen in soil and vine roots in harrowed and grass-covered vineyards. Agric. Ecosyst. Environ. 193, 70–82.
Albaladejo, J., Ortiz, R., Garcia-Franco, N., Ruiz Navarro, A., Almagro, M., Garcia Pintado, J., Martinez-Mena, M., 2013. Land use and climate change impacts on soil organic carbon stocks in semi-arid Spain. J. Soil Sediment 13, 265–277.
Alonso-Zarza, A., Dorado Valiño, M., Valdeolmillos Rodriguez, A., Ruiz Zapata, M.B., 2006. A recent analogue for palustrin carbonate environments: the Quaternary deposits of Las Tablas de Daimiel wetlands, Ciudad Real Spain. Geol. Soc. Am. Spec. Pap. 416, 153–168.
Amorosi, A., 2012. Chromium and nickel as indicators of source-to-sink sediment transfer in a Holocene alluvial and coastal system (Po Plain, Italy). Sediment. Geol. 280, 260–269.
Amorosi, A., Centineo, M.C., Dinelli, E., Lucchini, F., Tateo, F., 2002. Geochemical and mineralogical variations as indicators of provenance changes in Late Quaternary deposits of SE Po Plain. Sediment. Geol. 151, 273–292.
Amundson, R., Austin, A.T., Schuur, E.A.G., Yoo, K., Matzek, V., Kendall, C., Uebersax, A., Brenner, D., Baisden, W.T., 2003. Global Biogeochem. Cy. 17 (1), 1031. https://doi.org/10.1029/2002GB001903.
Bianchini, G., Laviano, R., Lovo, S., Vaccaro, C., 2002. Chemical?mineralogical characterisation of clay sediments around Ferrara (Italy): a tool for an environmental analysis. Appl. Clay Sci. 21, 165–176.
Bianchini, G., Natali, C., Di Giuseppe, D., Beccaluva, L., 2012. Heavy metals in soils and sedimentary deposits of the Padanian Plain (Ferrara, Northern Italy): characterisation and biomonitoring. J. Soil Sediment 12, 1145–1153.
Bianchini, G., Di Giuseppe, D., Natali, C., Beccaluva, L., 2013. Ophiolite inheritance in the Po plain sediments: insights on heavy metals distribution and risk assessment. Ofioliti 38, 1–14.
Bianchini, G., Cremonini, S., Di Giuseppe, D., Vianello, G., Vittori Antisari, L., 2014.

Multiproxy investigation of a Holocene sedimentary sequence near Ferrara (Italy): clues on the physiographic evolution of the eastern Padanian Plain. J. Soil Sediment 14, 230–242.
Bondesan, M., Favero, V., Viñals, M.J., 1995. New evidence on the evolution of the Po Delta coastal plain during the Holocene. Quat. Int. 29/30, 105–110.
Brodie, C.R., Leng, M.J., Casford, J.S.L., Kendrick, C.P., Lloyd, J.M., Yongqiang, Z., Bird, M.I., 2011. Evidence for bias in C and N concentrations and δ13C composition of terrestrial and aquatic organic materials due to pre-analysis acid preparation methods. Chem. Geol. 282, 67–83.
Caschetto, M., Colombani, N., Mastrocicco, M., Petitta, M., Aravena, R., 2017. Nitrogen and sulphur cycling in the saline coastal aquifer of Ferrara, Italy. A multi-isotope approach. Appl. Geochem. 76, 88–98.
Ciavatta, C., Govi, M., Vittori Antisari, L., Sequi, P., 1990. Characterization of humified compounds by extraction and fractionation on solid polyvynilpyrrolidone. J. Chromatogr. 509, 141–146.
Colombani, N., Salemi, E., Mastrocicco, M., Castaldelli, G., 2011. Groundwater nitrogen speciation in intensively cultivated lowland areas. In: Lambrakis, N., Stournaras, G., Katsanou, K. (Eds.), Advances in the Research of Aquatic Environment. Springer, Berlin, pp. 291–298.
DeNiro, M.J., Epstein, S., 1978. Influence of diet on the distribution of carbon isotopes in animals. Geochim. Cosmochim. Acta 42, 495–506.
Dauer, J.M., Perakis, S.S., 2014. Calcium oxalate contribution to calcium cycling in forest of contrasting nutrient status. For. Ecol. Manag. 334, 64–73.
De Clercq, T., Heiling, M., Dercon, G., Resch, C., Aigner, M., Mayer, L., Mao, Y., Elsen, A., Steier, P., Leifeld, J., Merckx, R., 2015. Predicting soil organic matter stability in agricultural fields through carbon and nitrogen stable isotopes. Soil Biol. Biochem. 88, 29–38.
Di Giuseppe, D., Bianchini, G., Faccini, B., Coltorti, M., 2014a. Combination of wavelength dispersive X-ray fluorescence analysis and multivariate statistic for alluvial soils classification: a case study from the Padanian Plain (Northern Italy). X-ray Spectrom. 43, 165–174.
Di Giuseppe, D., Bianchini, G., Vittori Antisari, L., Martucci, A., Natali, C., Beccaluva, L., 2014b. Geochemical characterization and biomonitoring of reclaimed soils in the Po River Delta (northern Italy): implications for the agricultural activities. Environ. Monit. Assess. 186, 2925–2940.
Di Giuseppe, D., Faccini, B., Mastrocicco, M., Colombani, N., Coltorti, M., 2014c. Reclamation influence and background geochemistry of neutral saline soils in the Po River Delta plain (Northern Italy). Environ. Earth Sci. 72, 2457–2473.
Di Giuseppe, D., Vittori Antisari, L., Ferronato, C., Bianchini, G., 2014d. New insights on mobility and bioavailability of heavy metals in soils of the Padanian alluvial plain (Ferrara Province, northern Italy). Chem. Erde Geochem. 74, 615–623.
Dunagan, S.P., Turner, C.E., 2004. Regional paleohydrologic and paleoclimatic setting of wetland/lacustrine depositional systems in the Morrison Formation (Upper Jurassic), Western Interior, USA. Sediment. Geol. 167, 269–296.
Dutta, K., Schuur, E.A.G., Neff, J.C., Zimov, S.A., 2006. Potential carbon release from permafrost soils of Northeastern Siberia. Global Change Biol. Bioenergy 12, 1–16.
Gonfiantini, R., Stichler, W., Rozanski, K., 1995. Standards and intercomparison materials distributed by the International atomic energy agency for stable isotope measurements. In: Stichler, W. (Ed.), Reference and Intercomparison Materials for Stable Isotopes of Light Elements. IAEA, Vienna, pp. 13–29 1993.
Hooijer, A., Page, S., Canadell, J.G., Silvius, M., Kwadijik, J., Wosten, H., Jauhiainen, J., 2010. Current and future CO_2 emissions from drained peatland in Southeast Asia. Biogeosciences 7, 1505–1514.
Johnson, K., Purvis, G., Lopez-Capel, E., Peacock, C., Gray, N., Wagner, T., März, C., Bowen, L., Ojeda, J., Finlay, N., Robertson, S., Worrall, F., Greenwell, C., 2015. Towards a mechanistic understanding of carbon stabilization in manganese oxides. Nat. Commun. 6, 7628.
Kovda, I., Morgun, E., Gongalski, K., 2014. Stable isotopic composition of carbonate pedofeatures in soils along a transect in the southern part of European Russia. Catena 112, 56–64.
Kusaka, S., Nakano, T., 2014. Carbon and oxygen isotope ratios and their temperature dependence in carbonate and tooth enamel using GasBench II preparation device. Rapid Commun. Mass Spectrom. 28, 563–567.
Lawrence, C.R., Harden, J.W., Xu, X., Schulz, M.S., Trumbore, S.E., 2015. Long-term controls on soil organic carbon with depth and time: a case study from the Cowlitz River Chronosequence, WA USA. Geoderma 247-248, 73–87.
Migani, F., Borghesi, F., Dinelli, E., 2015. Geochemical characterization of surface sediments from the northern Adriatic wetlands around the Po river delta. Part I: bulk composition and relation to local background. J. Geochem. Explor. 156, 72–88.
Millière, L., Hasinger, O., Bindschedler, S., Cailleau, G., Spangenberg, J.E., Verrecchia, E.P., 2011. Stable carbon and oxygen isotope signatures of pedogenic needle fibre calcite. Geoderma 161, 74–87.
Natali, C., Bianchini, G., 2014. Understanding the carbon isotopic signature in complex environmental matrices. Int. J. Environ. Qual. 14, 19–30.
Natali, C., Bianchini, G., 2015. Thermally based isotopic speciation of carbon in complex matrices: a tool for environmental investigation. Environ. Sci. Pollut. R. 22, 12162–12173.
Natali, C., Bianchini, G., Vittori Antisari, L., 2018. Thermal separation coupled with elemental and isotopic analysis: a method for soil carbon characterization. Catena 164, 150–157.
Oertel, C., Matschullat, J., Zurba, K., Zimmermann, F., 2016. Greenhouse gas emissions from soils – a review. Chem. Erde Geochem. 76 327-3.
Ogrinc, N., Kanduč, T., Krajnc, B., Vilhar, U., Simončič, P., Jin, L., 2015. Inorganic and organic carbon dynamics in forested soils developed on contrasting geology in Sloveniača stable isotope approach. J. Soil Sediment 16, 382–395.
Paul, 2014. Soil Microbiology, Ecology and Biochemistry, 4th edition. Academic press, pp. 598.
Rumpel, C., Kögel-Knabner, I., 2010. Deep soil organic matter—a key but poorly understood component of terrestrial C cycle. Plant Soil 338, 143–158.
Schlacher, T.A., Connolly, R.M., 2014. Effects of acid treatment on carbon and nitrogen stable isotope ratios in ecological samples: a review and synthesis. Methods Ecol. Evol. 5, 541–550.
Serrano, O., Serrano, L., Mateo, M.A., Colombini, I., Chelazzi, L., Gagnarli, E., Fallaci, M., 2008. Acid washing effect on elemental and isotopic composition of whole beach arthropods: implications for food web studies using stable isotopes. Acta Oecol. Montrouge (Montrouge) 34, 89–96.
Simeoni, U., Corbau, C., 2009. A review of the Delta Po evolution (Italy) related to climatic changes and human impacts. Geomorphology 107, 64–71.
Six, J., Conant, R.T., Paul, E.A., Paustian, K., 2002. Stabilization mechanisms of soil organic matter: implications for C-saturation of soils. Plant Soil 241, 155–176.
Soil Survey Staff -SSS, 2010. Keys to Soil Taxonomy, Eleventh edition. USDA, Natural Resources Conservation Service, pp. 338.
Stefani, M., Vincenzi, S., 2005. The interplay of eustasy, climate and human activity in the late Quaternary depositional evolution and sedimentary architecture of the Po Delta system. Mar. Geol. 222–223, 19–48.
Stevenson, F.J., Cole, M.A., 1999. Cycles of Soils: Carbon, Nitrogen, Phosphorus, Sulfur, Micronutrients, Second edition. John Wiley and Sons, New York, pp. 448.
Ungaro, F., Ragazzi, F., Cappelin, R., Giandon, P., 2008. Arsenic concentration in the soils of the Brenta plain (Northern Italy): mapping the probability of exceeding contamination thresholds. J. Geochem. Explor. 96 117–13.
Vittori Antisari, L., Dell'Abate, M.T., Buscaroli, A., Gherardi, M., Nisini, L., Vianello, G., 2010. Role of soil organic matter characteristics in a pedological survey: “Bosco Frattona” natural reserve (Site of Community Importance, Italy) case study. Geoderma 156, 302–315.
Wynn, J.G., Harden, J.W., Fries, T.L., 2006. Stable carbon isotope depth profiles and soil organic carbon dynamics in the lower Mississippi Basin. Geoderma 131, 89–109.
Zamanian, K., Pustovoytov, K., Kuzyakov, Y., 2016. Pedogenic carbonates: forms and formation processes. Earth Sci. Rev. 157, 1–17.